



# Analytical investigation and performance optimization of a three fluid heat exchanger with helical coil insertion for simultaneous space heating and water heating

Taraprasad Mohapatra<sup>1,2</sup> · Biranchi N. Padhi<sup>2</sup> · Sudhansu S. Sahoo<sup>3</sup>

Received: 3 November 2017 / Accepted: 5 December 2018 / Published online: 3 January 2019  
© Springer-Verlag GmbH Germany, part of Springer Nature 2019

## Abstract

In this paper, a three fluid heat exchanger is analytically modeled in order to predict the effects of different design parameters on its thermal performances. The optimum values of these parameters relating to maximum heat transfer and minimum pressure drop are assessed using Taguchi based optimization technique. The present heat exchanger is an improvement of double tube heat exchanger, where a helical coil is inserted in the annular space occupied in between two straight tubes. It is different from other three fluid heat exchangers with respect to construction, flow arrangement and thermal communication point of view, where the hot water is flowing through the helical coil as the heating fluid and continuously transferring thermal energy to normal water and air, which are flowing, in outer annulus and innermost straight tube. The results of the analytical approach are compared and validated against literature and good conformity between them is observed. The temperature distributions of three different fluids along the length of the present heat exchanger are assessed analytically for different flow configurations. Three different non-dimensional design parameters i.e. curvature ratio, non dimensional coil pitch and coil side Reynolds number are selected and their effect on heat transfer and pressure drop characteristics i.e. coil side Nusselt number, effectiveness and friction factor respectively are assessed. It is found that, for tube size 0.0045 m, coil pitch 0.013 m, coil diameter 0.04253 m and hot water flow rate 5 liters per minute, present heat exchanger will perform optimum. It is also resulted that, volumetric flow rate of hot water is the most effective parameter affecting heat transfer with a contribution ratio of 66.82% and tube size is the most effective parameters affecting pressure drop with a contribution ratio of 71.07%.

## Nomenclature

$A$	Surface area, $m^2$
$A_i$	Surface area of innermost tube, $m^2$
$B$	Diameter of innermost tube, m
$c_p$	Specific heat, $kJ/kg\cdot K$
$C$	Diameter of outermost tube, m
$C_1$	Intercept
$C_2$	Constant, $1/(Slope \times A_{c,i})$
$C_p$	Heat capacity, $kJ/K$
CV	Control volume

$d_c$	Diameter of helical tube, m
$D_c$	Coil diameter, m
$D_e$	Equivalent diameter
$De$	Dean number
$f$	Friction factor
$h$	Convective heat transfer co-efficient, $W/m^2\cdot K$
$k$	Thermal conductivity, $W/m\cdot K$
$L$	Length, m
$\dot{m}$	Mass flow rate, $kg/s$
$N$	Number of turns
$Nu$	Nusselt number
$p$	Pitch of helical coil, m
$Pr$	Prandtl number
$Q'$	Rate of heat transfer, $W$
$R$	Resistance
$Re$	Reynolds number
$T$	Temperature, $^\circ C$
$U$	Overall heat transfer co-efficient, $W/m^2\cdot K$
$V$	Velocity, $m/s$
$V^\infty$	Volume, $m^3$
$\dot{V}$	Volumetric flow rate, $m^3/s$

✉ Sudhansu S. Sahoo  
sahoo.sudhansu@gmail.com; sudhansu@cet.edu.in

<sup>1</sup> Department of Mechanical Engineering, C. V. Raman College of Engineering, Bhubaneswar, India

<sup>2</sup> Department of Mechanical Engineering, IIIT, Bhubaneswar, India

<sup>3</sup> Department of Mechanical Engineering, College of Engineering and Technology, Bhubaneswar, India

**Greek symbols**

$\rho$	Density, kg/m <sup>3</sup>
$\varepsilon$	Effectiveness
$\mu$	viscosity, N-s/m <sup>2</sup>
$\delta$	Curvature ratio, $d_c, i/D_c$
$\lambda$	Non-dimensional coil pitch, $p/\pi D_c$

**Subscripts**

<i>l</i>	Inlet
<i>2</i>	Outlet
<i>a</i>	Air
<i>act</i>	Actual
<i>ann</i>	Annulus
<i>c</i>	Coil
<i>cr</i>	Critical
<i>cu</i>	Copper
<i>e</i>	Equivalent
<i>f</i>	Fluid
<i>h</i>	Hot water
<i>i</i>	Inner
<i>L</i>	Larger
<i>m</i>	mean
<i>max</i>	Maximum
<i>min</i>	Minimum
<i>n</i>	Normal water
<i>o</i>	Outer
<i>ov</i>	Overall
<i>S</i>	Smaller
<i>TS</i>	Test section
<i>w</i>	Wall

**Superscripts**

<i>n</i>	Velocity exponent
----------	-------------------

**Abbreviations**

DOE	Design of experiments
LPM	Litre per minute
NTU	Numbers of transfer unit
SNR	Signal to noise ratio

**1 Introduction**

In many industrial processes, heat exchangers are the major components and having extensive application in process industries, Heating, Ventilation, Air conditioning and Refrigeration (HVAC & R), chemical plants, food industries, petroleum refineries etc. Recently researchers emphasize on the development of energy efficient, low cost and maintenance free heat exchangers with improved performance. So, heat exchangers manufactured these days are incorporated with numbers of heat transfer enhancement techniques, where types of flow, type of construction, way of contact between the fluids, product specifications, various physical characteristics of the fluid and the material are taken into consideration. Helical coil heat exchangers, compact heat exchangers, plate

fin heat exchangers, spiral heat exchangers, three fluid heat exchangers etc. are most commonly used heat exchangers these days, where different optimized techniques are used for heat transfer enhancement.

Experimental study on helically coiled tube heat exchangers for three different coil pitches, curvature ratio and use of Wilson plot method to determine heat transfer coefficients was found in literature [1]. It was reported that the shell side heat transfer coefficients of the coils for larger pitches are more effective than the ones with smaller pitches and heat transfer rates in counter flow configuration were more than parallel flow configuration. More generic way of calculating overall heat transfer coefficients in a triple tube heat exchanger has been developed by Batmaz and Sandeep [2]. Consequently, temperature profiles of all streams in the above heat exchanger in the axial direction were determined analytically. Rennie and Raghavan [3] experimentally studied the effect of mass flow rate on performance of a double-pipe helical heat exchanger for both flow configurations. Convective heat transfer coefficients were calculated by Wilson plots method. Tube side and annulus side Nusselt numbers were calculated and compared with numerical data. For larger coil, experimental data fit with numerical data but for smaller coil, some deviation is reported for the nature of the Wilson plots. Experimental study on isothermal steady state and non-isothermal unsteady state conditions in helical coils for Newtonian as well as for non-Newtonian fluids has been mentioned [4]. An innovative technique was used to correlate Nusselt number with dimensionless number, 'M', Prandtl number and coil curvature ratio. Several Nusselt number correlations were developed and good agreements between results were reported when compared with the literature. Zhang et al. [5] studied numerically the performance of a fin tube three fluid heat exchanger for different working conditions and circuit arrangements. Circuit arrangement has significant effect on the performance heat exchanger was reported. The heat transfer rate of all three fluids increases with increased mass flow rate of the hot fluid, inner tube diameter, inlet pressure of the hot fluid. Numerical model of predicting outlet temperatures in a triple concentric tube heat exchanger has been developed by [6]. Based on the validation with experimental data, the obtained model has been practically tested to cool a petroleum product with water in a triple concentric-tube heat exchanger. Steady and unsteady thermal behavior of triple concentric-tube heat exchanger with parallel and counter flow arrangements has been carried out using the finite difference method [7]. It was found that the fluids have a time lag and response of a triple concentric-tube heat exchanger in parallel flow configuration is faster than those of a counter flow arrangement. Effect of geometrical parameters of the shell and helically coiled tube heat exchangers has been established on heat transfer rate and entropy generation [8]. Optimal values of these parameters were obtained relative to

COD (heat transfer rate per entropy generation) minimized and maximized condition. Review on double pipe heat exchangers related to information about the development procedure, adopted heat transfer enhancement methods, use of nanofluids and their effect on performance in double pipe heat exchangers were reported in details [9]. Effects of flow rate, thermodynamic and geometrical parameters on exergetic characteristics (exergy loss, dimensionless exergy loss and second law efficiency) in a tube-in-tube helically coiled heat exchanger has been mentioned in detail using experimental techniques [10]. Enhancement in hot or cold water flow rates, hot water inlet temperature and coil diameter increases the amount of exergy loss was noted. It was reported that maximum exergy loss occurs in parallel flow configuration and exergy loss is negligibly affected by coil pitch. Experimental and numerical investigations of the performance characteristics of the triple concentric tube heat exchanger with inserted ribs have been carried out [11]. The effect of water mass flow rate, flow pattern, temperature variation, rib height and rib pitch on performance of the heat exchanger were assessed and a significant enhancement of the convective heat transfer occurs by the insertion of ribs to the inner annulus was reported.

Recently numerous research works are carried out to produce more efficient heat exchangers by employing various heat transfer enhancement techniques. One of the technique was stated by Unal [12, 13] that by introducing an intermediate tube (may be straight or helical tube) to the double tube heat exchangers, an efficient heat exchanger i.e. triple tube or three fluid heat exchanger will be formed, the effective length of heat exchanger will be reduced, larger heat exchanger area per unit length and better heat transfer co-efficient will be offered. Using the said technique numerous three fluid or triple tube heat exchangers were formed and their performances were investigated experimentally, analytically and numerically. Similar technique is adopted in this study i.e. the present TFHE is practically a double tube heat exchanger and a helical coil is inserted into the outer annular space for better performance. The helical tube is preferred in the present TFHE for insertion in place of straight tube because helical tube possesses certain advantages over straight tube i.e. better heat transfer rate due to more exposed surface area and created turbulence, shorter heat exchanger length and saving in material and cost.

Mohapatra et al. [14] experimentally investigated convective heat transfer of a helical coil insertion type three fluid heat exchanger used for simultaneous space and water heating purpose. The effects of variation of mass flow rate on performance of the TFHE were assessed. Seculic and Shah [15] presented a review paper on three fluid heat exchangers exist in literature and provided adequate information about their varieties and classifications with respect to various characteristics such as thermal communication, construction and flow arrangement. Thermal design aspects of three fluid heat exchangers,

development of dimensionless groups and their application in mathematical model formulation are explained in details.

It may be stated from literature review that numerous research papers were published on performance analysis and optimization of shell and coiled tube heat exchanger, tube in tube helical coil heat exchanger, heat exchanger tube with wire insertion, Three-fluid heat exchangers regarding two thermal communications and three thermal communications. However, relatively less information available regarding performance analysis of a three fluid heat exchanger (TFHE) with helical coil insertion. Hence, an analytical investigation and performance optimization of the present TFHE are aimed in this paper for better prediction of its space and water heating performance. Analytical model of the present TFHE is prepared, compared and validated against experimental results and other researchers mentioned in literature. The construction, flow arrangements and thermal communication associated with the TFHE presented in this paper are novel and require an exhaustive study. Taguchi based optimization method has been employed in this work is another novelty for determination of optimal design parameters towards performance enhancement of TFHE. The present TFHE may be used for simultaneous space and water heating purposes. In following sections, the details of analytical model, Taguchi method and performance optimization of the TFHE are explained.

## 2 TFHE test section

The schematic layout of the TFHE test section used in this study for the analytical modeling is depicted in Fig. 1. The length of the test section is 1.8 m. It consists two concentric parallel straight tubes and one helical coil. Outermost straight tube length is 1.8 m, internal diameter is 0.07 m, thickness is 0.0025 m, made up of G.I. pipe and insulated outside. Similarly innermost straight tube length is 1.8 m, internal diameter is 0.0268 m and thickness is 0.001 m made up of copper. The helical coil is inserted into the annular space occupied between two concentric parallel straight tubes in such a manner that the distances of the helical coil from both of the tubes are same. Helical coil is made up of copper. But the specification of the helical coil is not kept constant and varied during the study with respect to changes in dimensionless design parameters such as curvature ratio and non-dimensional pitch.

In TFHE test section, hot water is flowing through the helical coil, which transfers heat energy to normal water and air successively. Normal water is flowing through the outer annulus, which is the intermediate fluid medium of heat transfer between hot water and air. Air is flowing through the inner most copper tube.

In previously published experimental work [14], Flow control valves were connected along the passages of hot water,

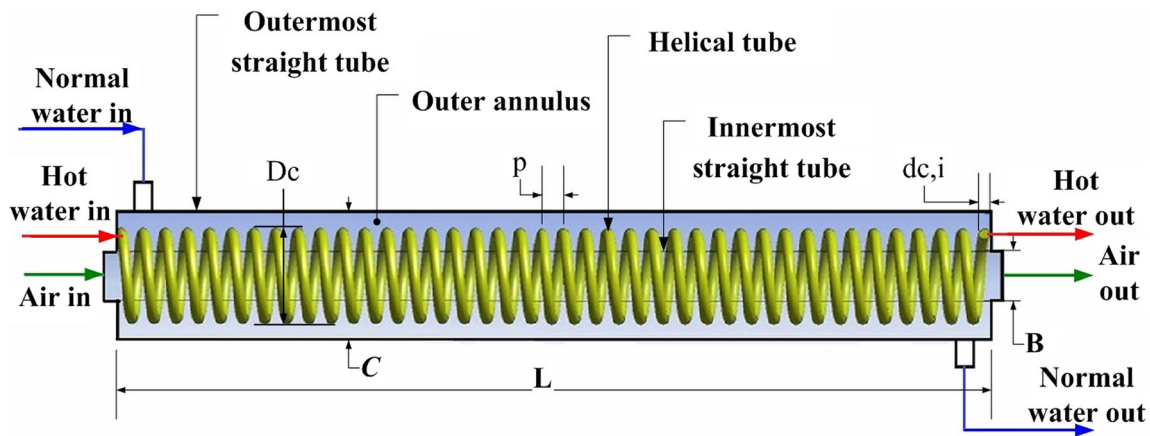


Fig. 1 Schematic layout of the TFHE test section

normal water and air to regulate the flow rate of these fluids. Rotameter were connected along the passages of hot and normal water to measure flow rate of both fluids. Anemometer was used to measure air velocity. Inside test section, 4 K-type thermocouples were attached at four different positions along the passages each fluid to measure inlet, two intermediate and outlet temperatures. Through the TFHE test section, hot water is supplied by a 0.5 HP centrifugal pump from a tank equipped with an immersion heater and thermostat, where as normal water is directly supplied from an overhead tank and air is supplied by a blower.

In the present study, identical values of various design parameters of the previously published experimental work [14] are employed in the analytical model as the input variables. Based on that, different output responses are obtained, as the exit temperatures of three different fluids and their corresponding thermo physical properties are determined analytically instead of experimentally. The analytical modelling and technique used for determination of the exit temperatures of different fluids at the outlet of the TFHE using control volume approach is mentioned in following section.

### 3 Analytical model

In this study, temperature distribution and performance optimization of the TFHE are conducted using an analytical model. Following formulae are used to prepare an analytical model from the experimental work.

#### 3.1 Mean temperature

$$\text{Mean temperature of hot water, } T_{h,m} = \frac{T_{h,1} + T_{h,2}}{2} \quad (1)$$

$$\text{Mean temperature of normal water, } T_{n,m} = \frac{T_{n,1} + T_{n,2}}{2} \quad (2)$$

$$\text{Mean temperature of air, } T_{a,m} = \frac{T_{a,1} + T_{a,2}}{2} \quad (3)$$

#### 3.2 Mass flow rate

$$\text{Mass flow rate of hot water, } \dot{m}_h = \rho_h \cdot \dot{V}_h \quad (4)$$

$$\text{Mass flow rate of normal water, } \dot{m}_n = \rho_n \cdot \dot{V}_n \quad (5)$$

$$\text{Mass flow rate of air, } \dot{m}_a = \rho_a \cdot \dot{V}_a \quad (6)$$

#### 3.3 Heat transfer rate

$$\text{Hot water heat rejection rate, } \dot{Q}_h = \dot{m}_h \cdot c_{ph} \cdot (T_{h,1} - T_{h,2}) \quad (7)$$

$$\text{Normal water heat gain rate, } \dot{Q}_n = \dot{m}_n \cdot c_{pn} \cdot (T_{n,2} - T_{n,1}) \quad (8)$$

$$\text{Air heat gain rate, } \dot{Q}_a = \dot{m}_a \cdot c_{pa} \cdot (T_{a,2} - T_{a,1}) \quad (9)$$

#### 3.4 Reynolds number

$$\text{Hot water Reynolds number, } Re_h = \frac{\rho_h \cdot V_h \cdot d_{c,i}}{\mu_h} \quad (10)$$

$$\text{Critical Reynolds number [16] of hot water, } Re_{cr} = 2 \times 10^4 \times \left( \frac{d_{c,i}}{D_c} \right)^{0.32} \quad (11)$$

$$\text{Normal water Reynolds number, } Re_n = \frac{\rho_n \cdot V_n \cdot D_e}{\mu_n} \quad (12)$$

$$\text{Air Reynolds number, } Re_a = \frac{\rho_a \cdot V_a \cdot B_i}{\mu_a} \quad (13)$$

Critical Reynolds number for innermost straight tube side fluid i.e. air is considered in this study as 2300.

### 3.5 Convective heat transfer coefficient

Wilson plot technique was used to calculate convective heat transfer coefficients inside and outside the helical tube by as explained by Rose [17]. Wilson plots allow the heat transfer coefficients to be calculated based on the overall temperature difference and the rate of heat transfer, neglecting the effect of wall temperatures. Wilson plots are generated by calculating the overall thermal resistance,  $R_{ov}$  against  $\frac{1}{V_f}$  for a number of trials, where flow velocity of one fluid is kept constant during the variation of flow velocity,  $V_f$  of other fluid. Overall thermal resistance,  $R_{ov}$  can be determined as  $1/UA$ . In this study, convective heat transfer coefficients for hot water,  $h_h$  is calculated by changing the flow rate of hot water inside the helical tube and keeping normal water flow rate constant in the outer annulus. The tube side heat transfer coefficient is assumed to behave in the following manner with the fluid velocity in the helical tube,  $V_h$ .

$$h_h = C_2 \cdot V_h^n \quad (14)$$

Where  $C_2$  is a constant,  $V_h$  is the velocity of hot water inside the helical tube and  $n$  is velocity exponent can be taken as 0.8 for turbulent flow.

Heat transfer coefficients of normal water,  $h_n$  is calculated by following equation [17].

$$h_n = \frac{1}{(C_1 - R_w) \cdot A_{c,o}} \quad (15)$$

Where  $C_1$  is the intercept,  $\frac{1}{C_2 \cdot A_{c,i}}$  is the slope of the straight line plotted by Wilson plot method.

Heat transfer coefficients of air,  $h_a$  is calculated Nusselt number correlation provided by Gnielinsky [18].

$$Nu_a = 0.0214(Re_a^{0.8} - 100) \cdot Pr^{0.4} \left( 1 + \left( \frac{B_i}{L_{TS}} \right)^{\frac{2}{5}} \right) \quad (16)$$

### 3.6 Overall heat transfer coefficient

Overall heat transfer coefficient outside of the helical coil when heat transfer takes from hot water to normal water

$$\frac{1}{U_o} = \frac{d_{c,o}}{h_h \cdot d_{c,i}} + \frac{A_{c,o} \cdot \ln\left(\frac{d_{c,o}}{d_{c,i}}\right)}{2\pi k_{cu} L_c} + \frac{1}{h_n} \quad (17)$$

Overall heat transfer coefficient inside the innermost copper tube when heat transfer takes from normal water to air

$$\frac{1}{U_o} = \frac{B_i}{h_n \cdot B_o} + \frac{A_i \cdot \ln\left(\frac{B_i}{B_o}\right)}{2\pi k_{cu} L_{TS}} + \frac{1}{h_a} \quad (18)$$

### 3.7 Effectiveness

Effectiveness of heat transfer between different fluids is calculated by

$$\varepsilon = \frac{\dot{Q}_{act}}{\dot{Q}_{max}} \quad (19)$$

For heat transfer between hot water and normal water

$$\dot{Q}_{act} = C_{ph}(T_{h,1} - T_{h,2}) \quad (20)$$

$$\dot{Q}_{max} = C_{min}(T_{h,1} - T_{n,1}) \quad (21)$$

For heat transfer between hot and normal water

$$Q_{act} = C_{pa}(T_{a,2} - T_{a,1}) \quad (22)$$

$$Q_{max} = C_{min}(T_{n,1} - T_{a,1}) \quad (23)$$

### 3.8 Parametric study

The effects of change in geometrical parameters of the helical coil on performance of the TFHE are assessed using following formulae.

Length of the coil with  $N$  numbers of turn,  $L_c$

$$= N \times \sqrt{(\pi \cdot D_c)^2 + (p)^2} \quad (24)$$

$$\text{Volume of the coil, } V_c = \left(\frac{\pi}{4}\right) \cdot d_{c,o}^2 \cdot L_c \quad (25)$$

$$\text{Volume of the outer annulus, } V_{ann} = \left(\frac{\pi}{4}\right) \cdot (C^2 - B_o^2) \cdot p \cdot N \quad (26)$$

$$\text{Volume available for normal water flow, } V_n = (V_{ann} - V_c) \quad (27)$$

$$\text{Equivalent diameter, } D_e = \frac{4 \times V_n}{\pi \cdot d_{co} \cdot L_c} \quad (28)$$

### 3.9 Temperature distribution

In this study temperature distribution of three fluids along the non dimensional axial distance of the TFHE are determined from control volume approach. Total volume of the TFHE test section is divided into 10 control volumes, where first control volume is allocated at the inlet of the TFHE whose length is equal to 0.18 m as shown in Fig. 2.

At the inlet of the control volume temperature of three fluids are known and same as the temperature data determined from experiments i.e.  $T_{h,1} = 62.5$  °C,  $T_{n,1} = 32$  °C and

$T_{a,1} = 35 \text{ }^\circ\text{C}$ . Exit temperature of three fluids at the outlet of the control volume i.e.  $T_{h,2}$ ,  $T_{n,2}$  and  $T_{a,2}$  are initially guessed and calculated from the validated analytical model using Newton-Raphson method. 100 iterations, 0.0001 convergences and 5% tolerance are considered for this study with the use following constraint equations.

$$\dot{Q}_h = \dot{Q}_n + \dot{Q}_a \Rightarrow \dot{m}_h \cdot c_{ph} \cdot (T_{h,1} - T_{h,2}) = \dot{m}_n \cdot c_{pn} \cdot (T_{n,2} - T_{n,1}) + \dot{m}_a \cdot c_{pa} \cdot (T_{a,2} - T_{a,1}) \tag{29}$$

$$\dot{Q}_h = \dot{Q}_h \Rightarrow \dot{m}_h \cdot c_{ph} \cdot (T_{h,1} - T_{h,2}) = \varepsilon \cdot C_{\min} \cdot (T_{h,1} - T_{n,1}) \tag{30}$$

Effectiveness,  $\varepsilon =$  Effectiveness,  $\varepsilon$ .  
For parallel flow configuration

$$\Rightarrow \left( \frac{\dot{m}_h \cdot c_{ph} \cdot (T_{h,1} - T_{h,2})}{C_{p,\min} \cdot (T_{h,1} - T_{n,1})} \right) = \frac{1 - \exp\left(-NTU \cdot \left(1 + \frac{C_{p,\min}}{C_{p,\max}}\right)\right)}{\left(1 + \frac{C_{p,\min}}{C_{p,\max}}\right)} \tag{31}$$

For counter flow configuration

$$\Rightarrow \left( \frac{\dot{m}_h \cdot c_{ph} \cdot (T_{h,1} - T_{h,2})}{C_{p,\min} \cdot (T_{h,1} - T_{n,1})} \right) = \frac{1 - \exp\left(-NTU \cdot \left(1 - \frac{C_{p,\min}}{C_{p,\max}}\right)\right)}{1 - \left(\frac{C_{p,\min}}{C_{p,\max}}\right) \cdot \exp\left(-NTU \cdot \left(1 - \frac{C_{p,\min}}{C_{p,\max}}\right)\right)} \tag{32}$$

Then exit temperature data calculated from the first control volume are used as the inlet temperature data for the second control volume. The exit temperatures of three fluids for second and remaining eight control volumes are calculated in the similar procedure as adopted for first control volume. Fluid properties, which are used in above calculations are obtained based on the equations mentioned in Appendix.

### 3.10 Validation of experimental approach and analytical model

The results of the experimental approach and analytical model i.e. coil side Nusselt number of hot water,  $Nu_i$  and annulus side Nusselt number of normal water,  $Nu_o$  were verified with Nusselt numbers reported from literature for counter flow configuration and shown in (Figs. 3 and 4). There are numbers of Nusselt number correlations noted in literature and represented as a function of Dean number or Reynolds number or Helix number with Prandtl number for both the uniform heat flux and wall temperature boundary conditions. For verification and validation, the coil side Nusselt numbers,  $Nu_i$  were compared with the results of Nusselt number correlations presented by Kalb & Seader [21], Rogers & Mayhew [20] and Seban & McLaughlin [19]. Similarly, annulus side Nusselt numbers,  $Nu_o$  were compared with the results of Nusselt number correlations presented by Coates and Pressburg [23]. The Nusselt number correlations of different researchers were considered for validations are represented in Table 1. Good agreement between the results of previously published experimental work [14] and the current analytical model with the literature are observed. However, variations are seen as for as results based on other researchers are concerned. These variations may be due to the analysis of the present TFHE under different geometry, flow arrangements, boundary condition and thermal communications. The Nusselt number correlations presented in Table 1 from literature are merely suitable for either uniform heat flux or uniform wall temperature boundary condition. But the present work is associated with fluid to fluid heat transfer boundary condition, which is neither uniform heat flux nor uniform wall temperature boundary condition. Fluid to fluid heat transfer boundary condition was introduced by Rennie [3], where energy transfer takes place between two fluids are separated by a thin solid wall. Besides the thermal

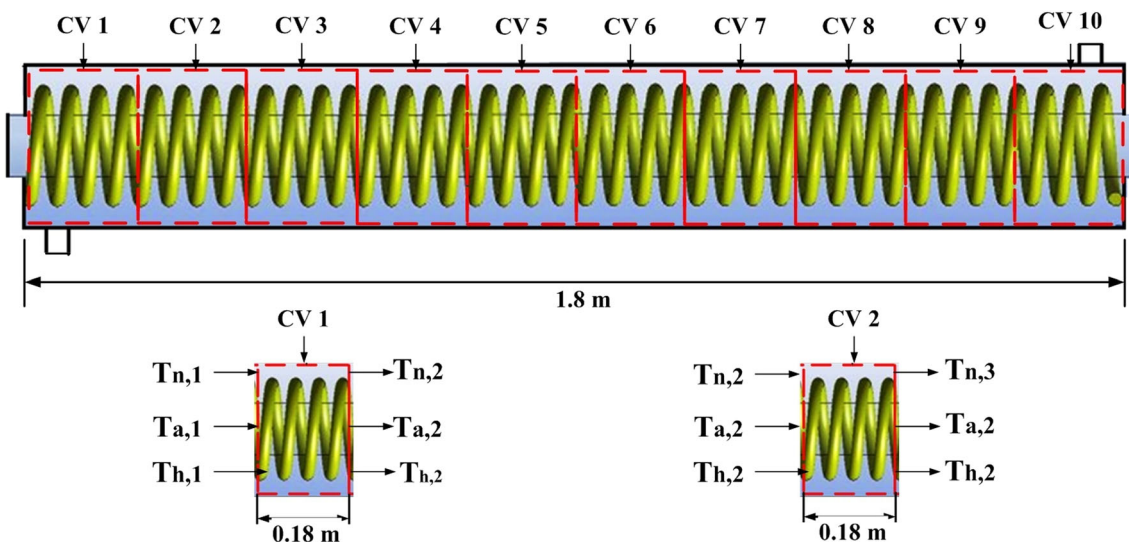


Fig. 2 Control volume approach for determination of analytical temperature distribution

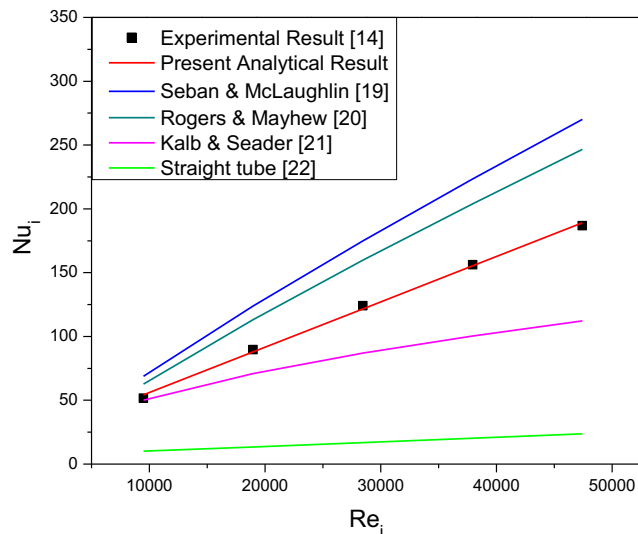


Fig. 3 Comparison of coil side Nusselt numbers with literature

energy transfer takes place from hot water to normal water and normal water to air in the present TFHE is associated with two thermal communications, whereas the Nusselt number correlations presented in Table 1 are suitably developed from energy transfer with one thermal communication.

Similarly, coil side friction factor,  $f_i$  was verified with friction factors reported in literature for counter flow configuration which is shown in Fig. 5. There are few friction factor correlations noted in literature as a function of Dean number, Reynolds number, curvature ratio of the helical coil. For verification and validation, the coil side friction factor,  $f_i$  was compared with the results of friction factor correlations presented by Mishra and Gupta [22], Blasius [24] along with associated friction factors for straight tube. The friction factor correlations of different researchers were considered for validations are represented in Table 1. Good agreement between the results of the experimental approach and analytical model

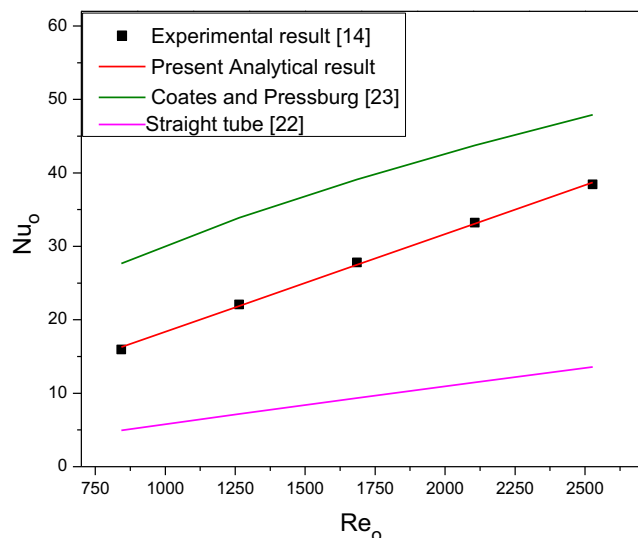


Fig. 4 Comparison of outer annulus side Nusselt numbers with literature

with literature are observed, however some variations in results are identified. The TFHE geometry, construction, flow arrangement, boundary condition and thermal communications associated with the present work may be the cause of this mismatch along with the use of helical tube of 21.26 m length, which is too long compared to others mentioned in literatures. It is worth mentioning that friction factor is more for helical tube case compared to straight tube assumptions.

#### 4 Taguchi method

These days various heat transfer enhancement techniques (i.e. active or passive techniques) are employed to produce more compact and efficient heat exchangers, resulting towards energy and material savings. Performance of TFHE can be enhanced appreciably by using a reasonable optimization approach. So many parameters affect the thermal performance of the TFHE and consideration of all these parameters for optimum result would increase the cost and time of experimentation. For optimum design, the principal factors are determined by Taguchi method, which reduce experimental costs. Jamshidi et al. [16] used Taguchi method to investigate the effect of fluid flow and geometrical parameters of a shell and coiled tube heat exchanger on heat transfer rate. Nine experiments were conducted and the optimum values of various design parameters for maximum heat transfer were obtained in the range of  $0.0813 < D_c < 0.116$ ,  $13 < p < 18$ , tube side and shell side flow rates from 1 to 4 LPM. Etghani and Baboli [25] used Taguchi approach to determine optimum levels of different design parameters for a shell and helical tube heat exchanger i.e. pitch coil, tube diameter, hot and cold flow rate for maximum heat transfer rate and minimum exergy loss. From result they reported that Nusselt number increases with increase in mass flow rate, tube diameter and decreases with increase in coil pitch. Gunes et al. [26] used Taguchi method to determine the optimum values of different design parameters for a tube with equilateral triangular cross-sectioned coiled wire inserts i.e. the ratio of the distance between the coiled wire and test tube wall to tube diameter ( $s/D$ ), pitch ratio ( $p/D$ ), ratio of the side length of equilateral triangle to tube diameter ( $a/D$ ) and Reynolds number ( $Re$ ) on maximum heat transfer (i.e. Nusselt number) and minimum pressure drop (i.e. friction factor). Contribution ratios for each parameter on the heat transfer and pressure drop were determined and  $s/D = 0.0357$ ,  $p/D = 1$ ,  $a/D = 0.0714$  and  $Re = 19,800$  were obtained optimum values for these design parameters. Jamshidi et al. [27] used Taguchi method to investigate the effect of fluid flow and geometrical parameters on JF factor. They conducted nine experiments and determined optimum design parameters for water and nano fluid subjected to constant temperature boundary condition in helical tube

**Table 1** Nusselt number and friction factor correlations considered for validation under different experimental condition

Author	Correlations	Experimental Conditions		
		Curvature ratio, $\delta = d_{ci}/D_c$	Dean number, $De$ or Reynolds number, $Re$	Prandtl Number, $Pr$
Nusselt number correlations:				
Rogers & Mayhew, 1964	$Nu_i = 0.023Re^{0.085}Pr^{0.4} \left(\frac{d_{ci}}{D_c}\right)^{0.1}$	0.0926, 0.075 and 0.05	10, 000 $\leq Re \leq$ 1, 00, 000	–
Kalb and Seader, 1972	$Nu_i = 0.913De^{0.476}Pr^{0.2}$	$0.01 \leq \delta \leq 0.1$	$80 \leq De \leq 1, 200$	$0.7 \leq Pr \leq 5$
	$Nu_i = 0.836De^{0.5}Pr^{0.1}$	$0.01 \leq \delta \leq 0.1$	$De \geq 1, 200$	$0.7 \leq Pr \leq 5$
Seban and McLaughlin, 1963	$Nu_i = 0.021Re^{0.85}Pr^{0.4} \left(\frac{d_{ci}}{D_c}\right)^{0.1}$	0.0096, 0.0588	6, 000 $\leq Re \leq$ 65, 000	$2.9 \leq Pr \leq 5.7$
Coates and Pressburg, 1959	$Nu_o = 0.6Re^{0.5}Pr^{0.31}$	–	$50 \leq Re \leq 10, 000$	–
Friction factor correlations:				
Mishra and Gupta, 1979	$f_i - f_s = \frac{0.0075}{\sqrt{\lambda}}$	$0.0029 \leq \delta \leq 0.15$	$4, 500 \leq Re \leq 10^5$	–
Blasius, 1972	$f_i = 0.3164Re^{-0.25}$	–	–	–

are  $D_c = 110$  mm,  $P_c = 21.4$  mm,  $\dot{m} = 0.016$ ,  $\varphi = 3\%$ . They noted that diameter of the coil,  $D_c$  have the highest contribution followed by pitch of the coil,  $p$  on optimal result.

Taguchi method is a standardized approach for determining the best combination of input parameters to get optimum result. This is accomplished through design of experiments (DOE). It provides a method for quantitatively identifying just the right parameters that go together for optimal performance or service. In literature, it is mentioned that Taguchi method is incorporated with three design stages i.e. system design, parameter design and tolerance design. In this paper, the optimum values of system parameters or thermal performance parameters i.e.  $U_o$  and  $\varepsilon$  are determined from parameter design stage. The variations in performance parameters are measured by signal to noise ratio i.e.  $SNR$  or  $S/N$  ratio, where  $S$  is the signal stands for mean and  $N$  is the noise stands for standard deviation in Taguchi approach. Three types of quality

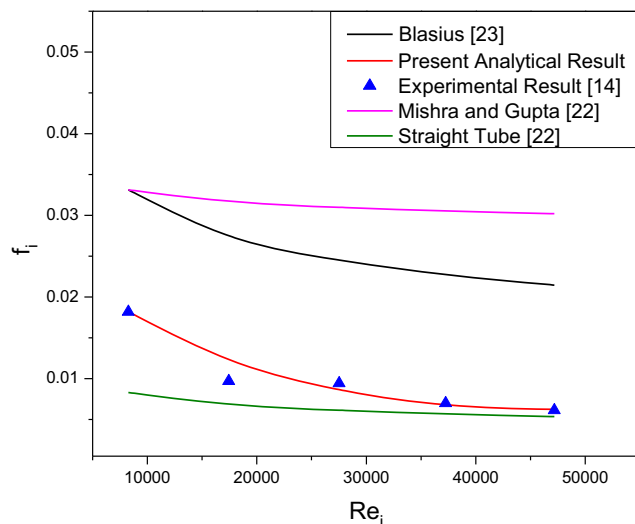
characteristics “larger is the better”; “nominal is the best” and “smaller is the better” are used to analyze  $S/N$  ratio. For the current study following five steps of Taguchi technique are used.

**Step 1 Identification of the objectives:** Determination of the optimum values of design parameters for maximum heat transfer and minimum pressure drop for the flow in TFHE is the objective of this work.

**Step 2 Selection of characteristics:** Nusselt number,  $Nu_i$  and friction factor,  $f$  are selected to analyze the thermal behavior and pressure drop characteristics of the TFHE. So in this study “larger is the better” quality characteristic is preferred for Nusselt number,  $Nu_i$  and “smaller is the better” quality characteristic is preferred for friction factor,  $f_i$ .

**Step 3 Selection of various factors and their levels:** Thermal performance and pressure drop characteristics of the TFHE are mostly affected by the geometrical parameters of the helical coil, volumetric flow rate and inlet temperature of three fluids etc. In this study, tube size ( $d_{ci}$ ), coil pitch ( $p$ ), coil diameter ( $D_c$ ), and volumetric flow rate of hot water ( $\dot{V}_h$ ) of the helical coil are selected as the control factors, temperature of normal water ( $T_n$ ) and air ( $T_a$ ) are selected as the noise factors for influencing heat transfer in the TFHE. The levels of control factors and noise factors are represented in Table 2.

**Step 4 Selection of an orthogonal array:** Taguchi method is well known for design of experiments by employing a standard table known as orthogonal array for study of various design parameters relative to single quality characteristics. The time required for experimental investigation can be reduced significantly by using special design orthogonal array. A suitable orthogonal array is selected depending on the number of factors with their levels,

**Fig. 5** Comparison of coil side friction factor with literature



**Table 2** Design factors and their levels

Control Factors	$d_{c,i}$ , m	$p$ , m	$D_c$ , m	$\dot{V}_h$ , LPM
Level 1	0.0045	0.013	0.04253	1
Level 2	0.008	0.018	0.0494	3
Level 3	0.01092	0.023	0.056266	5
Noise Factors	$T_a$ , °C	$T_n$ , °C		
Level 1	15	12		
Level 2	35	32		

degrees of freedom, objective of the study, available resources and budget with time constraints. Minitab 16.0 is used for the analysis and the interaction between the design parameters were neglected in this study. For four control factors with three levels, L9 orthogonal array and for two noise factors with two levels, L4 orthogonal array were generated and shown in Table 3.

In this study, noise factors are considered along with control factors, which are difficult or impractical to control. But Taguchi method provides good criterion for assessing the effect of noise factors by controlling these during experiments for carrying out a robust design and for better understanding of its effect on performance. So in this article two arrays are proposed, one for the control factors named as control array or inner array and other for the noise factors named as noise array or outer array, which are shown in Table 4.

**Step 5 Conduction of experiments and result analysis:** Orthogonal array design provides the idea about the number of experiments or test run to be conducted in Taguchi method analysis. In this study, these orthogonal arrays are generated in such a way that all the noise factors combination specified by outer L4 orthogonal array are run with every combination of the control factors specified by inner L9 orthogonal array and total 36 number of experiments or test run have to be performed with assessing the mean and S/N ratio of thermal performance and pressure drop characteristics of the TFHE. But conducting 36 test runs with 4 different noise factor conditions in 9 different heat exchanger test section is practically difficult, time consuming and costly. Therefore an analytical model of the present TFHE is prepared, compared and validated against experimental results [14] and literature. Afterwards the output responses i.e. Coil side Nusselt number and friction factor from 36 test runs were obtained from the validated analytical model for different noise factors and TFHE test sections without conducting the experiments in actual practice, which is also another uniqueness of this paper. Then all results of  $Nu_i$  and  $f_i$

obtained from analytical model are entered in Table 4 for the analysis.

The effect of helical coil design parameters on thermal performance characteristics of the TFHE are measured by  $SNR$  or  $S/N$  (signal to noise) ratio. For  $Nu_i$  and  $f_i$  following formulas were used during the analysis of  $SNR$  or  $S/N$  ratio for “larger is the better” and “smaller is the better” quality characteristics.

$$SNR_L = -10 \log_{10} \left( \frac{1}{Nu_i^2} \right) \quad (33)$$

$$SNR_S = -10 \log_{10} (f_i^2) \quad (34)$$

Higher value of  $S/N$  ratio indicates higher performance characteristics. So the optimum levels of various design parameters were obtained corresponding to the greatest value of  $S/N$  ratio reported in the Table 4. Depending on the  $S/N$  ratios, contribution ratios of all factors on thermal performance of the TFHE are calculated and shown in Table 4.

In this study, heat transfer from hot water to normal water was only considered for assessing the effect of optimum design parameters of the TFHE on Nusselt number and friction factor neglecting the effect of normal water on air. Because the helical coil was placed inside the outer annulus of the TFHE through which normal water was flowing, where as hot water was flowing through the helical coil. So any parametric changes and volumetric flow variation inside the helical coil would affect the quantity of heat transfer from hot water to normal water directly and indirectly affect airside performance. Air or inner annulus side performance is affected by

**Table 3** Orthogonal array for control and noise factors

L9 orthogonal array for control factors				
No.	$d_{c,i}$	$p$	$D_c$	$\dot{V}_h$
1	0.0045	0.013	0.04253	1
2	0.0045	0.018	0.0494	3
3	0.0045	0.023	0.056266	5
4	0.008	0.013	0.0494	5
5	0.008	0.018	0.056266	1
6	0.008	0.023	0.04253	3
7	0.010922	0.013	0.056266	3
8	0.010922	0.018	0.04253	5
9	0.010922	0.023	0.0494	1
L4 orthogonal array for noise factors				
No.	$T_a$	$T_n$		
1	15	12		
2	15	32		
3	35	12		
4	35	32		

**Table 4** Mean and S/N ratio of output responses

Mean and S/N ratio of coil side Nusselt number, $Nu_i$											
Outer Array (L4)					Ta <sub>1</sub>	15	15	35	35		
					Tn <sub>1</sub>	12	32	12	32		
Inner Array (L9)					Coil side Nusselt number, $Nu_i$				Responses		
RUN	d <sub>ci</sub>	P	D <sub>c</sub>	$\dot{V}_h$					Mean	S/N Ratio	
1	0.0045	0.013	0.04253	1	52.6953	55.3043	52.7488	55.2761	54.0061	34.6489	
2	0.0045	0.018	0.0494	3	120.376	124.908	120.376	124.862	121.887	41.7191	
3	0.0045	0.023	0.056266	5	171.718	178.167	171.718	124.908	161.628	44.1703	
4	0.008	0.013	0.0494	5	122.276	126.414	122.276	126.414	124.345	41.8926	
5	0.008	0.018	0.056266	1	37.8056	38.9703	37.8056	38.9703	38.3879	31.6839	
6	0.008	0.023	0.04253	3	89.3307	92.5619	89.3307	92.5619	90.9463	39.1757	
7	0.01092	0.013	0.056266	3	69.405	71.8145	69.405	71.8145	71.0113	37.0266	
8	0.01092	0.018	0.04253	5	105.448	109.265	105.448	109.265	107.357	40.6166	
9	0.01092	0.023	0.0494	1	32.9951	34.0565	32.9951	34.0565	33.5258	30.5076	
Mean and S/N ratio of coil side friction factor, $f_i$											
Outer Array (L4)					Ta <sub>1</sub>	15	15	35	35		
					Tn <sub>1</sub>	12	32	12	32		
Inner Array (L9)					Coil side Friction factor, $f_i$				Responses		
RUN	d <sub>ci</sub>	p	D <sub>c</sub>	$\dot{V}_h$					Mean	S/N Ratio	
1	0.0045	0.013	0.04253	1	0.0211	0.0211	0.0211	0.0211	0.0211	33.515	
2	0.0045	0.018	0.0494	3	0.0062	0.0106	0.0106	0.0106	0.0091	40.789	
3	0.0045	0.023	0.056266	5	0.011	0.0111	0.011	0.0111	0.011	39.135	
4	0.008	0.013	0.0494	5	0.1105	0.1108	0.1105	0.1108	0.1107	19.12	
5	0.008	0.018	0.056266	1	0.4461	0.4472	0.4461	0.4472	0.4467	7.0004	
6	0.008	0.023	0.04253	3	0.2404	0.241	0.2404	0.241	0.2407	12.371	
7	0.01092	0.013	0.056266	3	0.5642	0.5656	0.5642	0.5656	0.5651	4.9573	
8	0.01092	0.018	0.04253	5	0.7259	0.7277	0.7259	0.7277	0.7268	2.7716	
9	0.01092	0.023	0.0494	1	2.7019	2.7086	2.7019	2.7086	2.7053	-8.644	

normal water or outer annulus side performance and normal waterside performance could be enhanced by using the optimum design parameters of the TFHE determined by Taguchi method. This study is conducted with an assumption of increasing airside performance with an increase in normal waterside or outer annulus side performance.

## 5 Results and discussion

### 5.1 Analytical temperature distribution for different flow configurations

The analytical temperature distribution of three fluids i.e. hot water, normal water and air along the length of the TFHE test section were determined from the analytical model for different flow configurations are shown in Figs. 6, 7, 8 and 9.

Figure 6 represents the analytical temperature distribution of three fluids along the length of the TFHE for parallel flow configuration, where as Figs. 7, 8 and 9

represents the analytical temperature distribution of three fluids along the length of the TFHE test section for counter flow configurations for successive reversal of flow direction of hot water, normal water and air. For this study, hot water inlet temperature is 62.5 °C, normal water inlet temperature is 32 °C and air inlet temperature is 35 °C are taken in the validated analytical model for a fixed tube size, coil pitch, coil diameter, hot water, normal water and air mass flow rate. The TFHE presented here is used for simultaneous space heating and water heating by the hot water, which is flowing through the helical coil. Out of four flow configurations for space heating parallel flow configuration and for water heating counter flow configuration with normal water flow direction reversal can be adopted for optimum result. In Figs. 6, 7, 8 and 9, everywhere a cross over point between normal water and air is seen, because the air entered the TFHE at higher temperature than inlet temperature of normal water and the rate of rise in temperature of normal water is more compared to air.

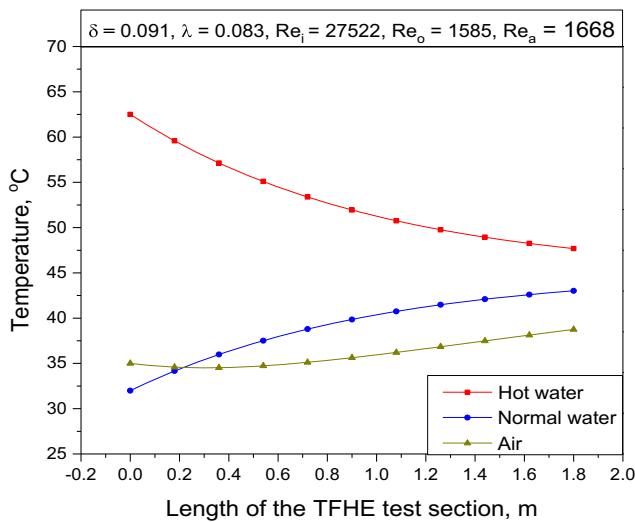


Fig. 6 Analytical temperature distribution of three fluids along the length of the TFHE for parallel flow configuration

### 5.2 Design parameters and thermal performance of the TFHE

Simultaneous space heating and water heating is the main objective of the present TFHE, where thermal energy transfers takes place from helical tube side fluid i.e. hot water to outer annulus fluid i.e. normal water and inner most tube fluid i.e. air. For better prediction of the heating performance of the TFHE, the performance of the TFHE is required to be investigated with respect to various design parameters. Hence three different non-dimensional design parameters i.e. curvature ratio, non dimensional coil pitch and coil side Reynolds number are selected for this study and their effect on two non-dimensional thermal performance of the TFHE i.e. coil side

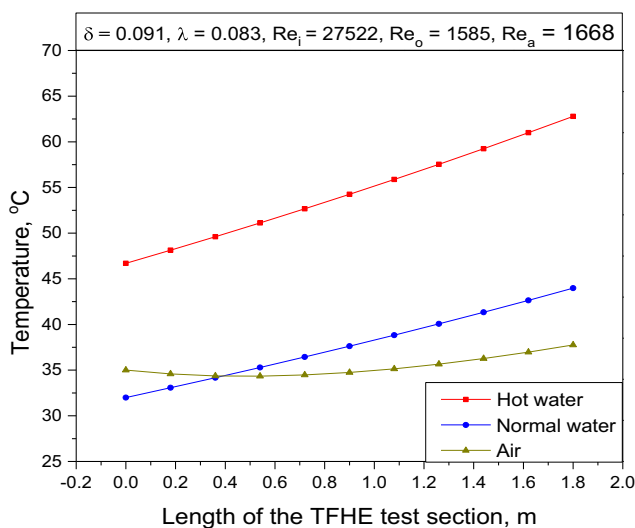


Fig. 7 Analytical temperature distribution of three fluids along the length of the TFHE for counter flow configuration, when hot water flow direction was only reversed

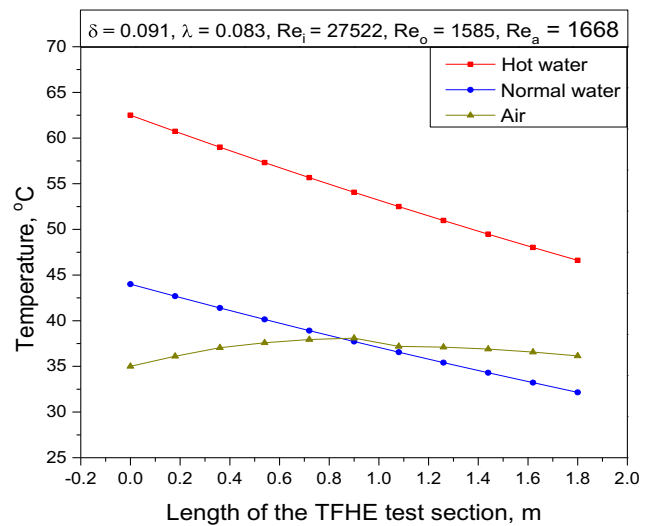


Fig. 8 Analytical temperature distribution of three fluids along the length of the TFHE for counter flow configuration, when normal water flow direction was only reversed

Nusselt number and effectiveness are assessed and presented as follows.

#### 5.2.1 The effect of coil curvature ratio on thermal performance of the TFHE

The effect of coil curvature ratio,  $\delta$  on thermal performance of the TFHE i.e. coil side Nusselt number,  $Nu_i$  and effectiveness,  $\epsilon$  are tested in the validated analytical model for three different coil curvature ratio i.e. 0.091, 0.152 and 0.216 and the results are illustrated in Fig. 10 for counter flow configuration with respect to coil1, coil 2 and coil 3. These coils are different from each other with respect to their coil diameter i.e. 0.04253, 0.0494 and 0.056266 m respectively.

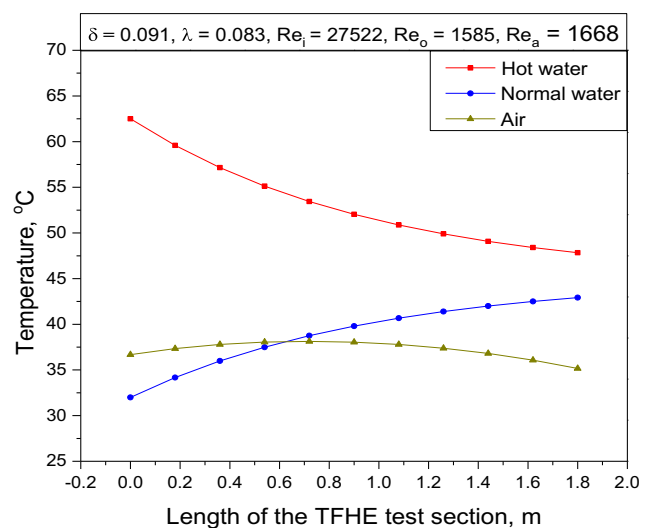


Fig. 9 Analytical temperature distribution of three fluids along the length of the TFHE for counter flow configuration, when air flow direction was only reversed

In this study, non-dimensional coil pitch,  $\lambda$ , coil side and outer annulus side volumetric flow rate are taken as constant with respect to variation or increase in coil curvature ratio. By increasing the curvature ratio of either coil 1 or coil 2 or coil 3, fluid velocity inside the helical tube decreases and related residence time increases for a particular volumetric flow rate of hot water. As a result, coil side Reynolds number, mean temperature of heat rejection and Prandtl number of hot water decreases, whereas the rate of heat rejection from hot water to normal water increases. As coil side Nusselt number is a function of coil side Reynolds number, Prandtl number and coil curvature ratio, therefore coil side Nusselt number decreases with decreased Reynolds number, Prandtl number and increased curvature ratio. Decreased coil side Nusselt number leads to decrease in coil side convective heat transfer coefficient, however outer annulus side convective heat transfer coefficient increases with increment in mean temperature of normal water. So, overall heat transfer coefficient, NTU and effectiveness of heat transfer from coil side fluid to outer annulus side fluid increases, which are in agreement with the result indicated in Fig. 10.

From Fig. 10, it is also observed that with increment in coil diameter associated with three different coils, effectiveness of heat transfer from coil side fluid to outer annulus side fluid

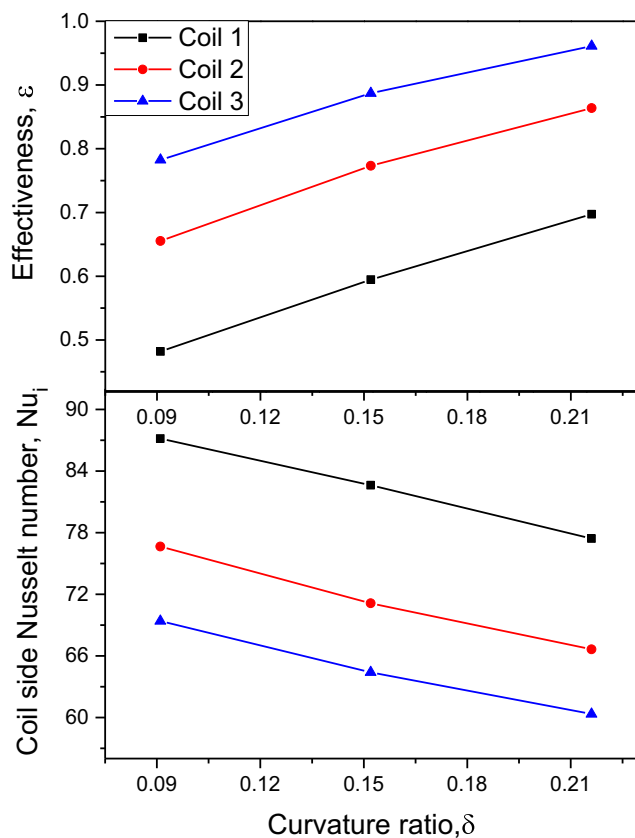


Fig. 10 Effect of coil curvature ratio on thermal performance of the TFHE

increases and coil side Nusselt number decreases. Because, increased coil diameters increases heat transfer surface area, heat rejection rate and residence time whereas mean temperature of heat rejection of hot water, coil side Reynolds number, Prandtl number and coil curvature ratio decreases. As a result, coil side Nusselt number decreases with decreased coil side Reynolds number, Prandtl number and curvature ratio. But at the same time, effectiveness increases with increased heat rejection rate from hot water to normal water.

### 5.2.2 The effect of non-dimensional coil pitch on thermal performance of the TFHE

The effect of non-dimensional coil pitch,  $\lambda$  on thermal performance of the TFHE i.e. coil side Nusselt number,  $Nu_i$  and effectiveness,  $\epsilon$  were tested in the validated analytical model for three different non-dimensional coil pitch i.e. 0.083, 0.115 and 0.148 and the results are illustrated in Fig. 11 for counter flow configuration with respect to coil 1, coil 2 and coil 3. These coils are different from each other with respect to their coil diameter i.e. 0.04253, 0.0494 and 0.056266 m respectively.

In this study, coil curvature ratio,  $\delta$ , coil side and outer annulus side volumetric flow rate are taken as constant with

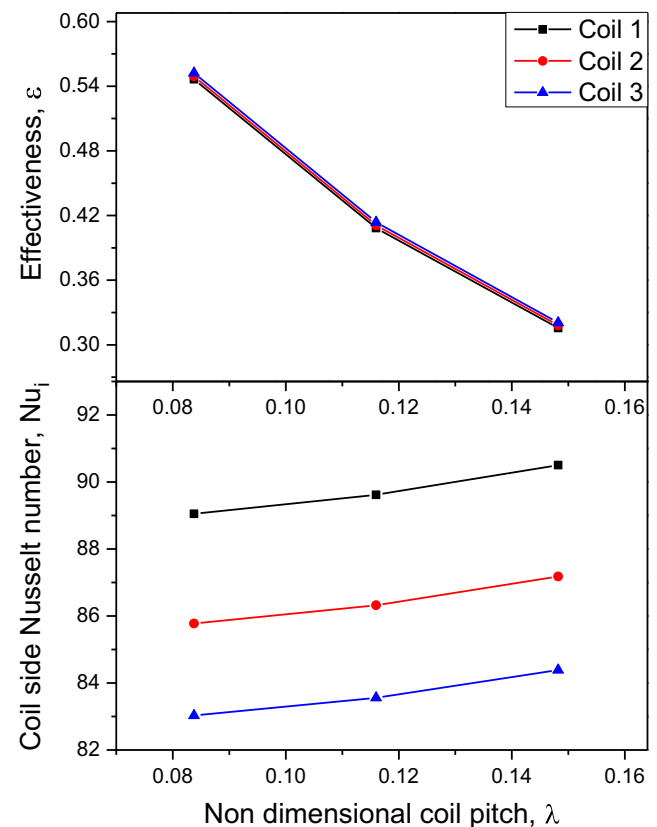


Fig. 11 Effect of non-dimensional coil pitch on thermal performance of the TFHE

respect to variation or increase in non-dimensional coil pitch. By increasing the non-dimensional coil pitches of either coil 1 or coil 2 or coil 3, number of turns of the helical coil, heat transfer surface area, coil side heat rejection rate and residence time decreases, whereas the coil side mean temperature of heat rejection of hot water, coil side Reynolds number and Prandtl number increases. As a result, for fixed curvature ratio coil side Nusselt number increases with increment in coil side Reynolds number and Prandtl number. So coil side convective heat transfer coefficient of hot water increases and annulus side convective heat transfer coefficient of normal water decreases due to drop in mean temperature of normal water. Therefore overall heat transfer coefficient, NTU and effectiveness of the TFHE decreases, which are in agreement with the result indicated in Fig. 11.

From Fig. 11, it is also observed that with increment in coil diameter associated with three different coils, effectiveness of heat transfer from coil side fluid to outer annulus side fluid increases negligibly and coil side Nusselt number decreases significantly. Because, increased coil diameters increases heat transfer surface area, heat rejection rate and residence time whereas mean temperature of heat rejection of hot water, coil side Reynolds number, prandtl number and coil curvature ratio decreases. As a result, coil side Nusselt number decreases with decreased coil side Reynolds number, Prandtl number and curvature ratio. But at the same time, effectiveness increases insignificantly with little increment in heat rejection rate from hot water to normal water.

### 5.2.3 The effect of coil side Reynolds number on thermal performance of the TFHE

The effect of coil side Reynolds number,  $Re_i$  on thermal performance of the TFHE i.e. coil side Nusselt number,  $Nu_i$  and effectiveness,  $\varepsilon$  were tested in the validated analytical model for three different coil side Reynolds number i.e. 9026, 29,467 and 50,276 and the results are illustrated in Fig. 12 for counter flow configuration with respect to three different outer annulus side Reynolds number,  $Re_o$  i.e. 779, 1154 and 1510 respectively.

In this study, coil curvature ratio,  $\delta$ , non-dimensional coil pitch,  $\lambda$  are taken as constant with respect to variation or increase in coil side Reynolds number. By increasing the coil side Reynolds number either in coil 1 or coil 2 or coil 3, velocity of hot water, mean temperature of heat rejection and Prandtl number increases, whereas residence time and the quantity of heat rejection from hot water to normal water decreases. As a result, for fixed curvature ratio, coil side Nusselt number increases with increased coil side Reynolds number and Prandtl number. Increased coil side Nusselt number increases coil side and outer annulus side convective heat transfer coefficient and overall heat transfer coefficient. But NTU decreases, because the rate of rise in overall heat transfer

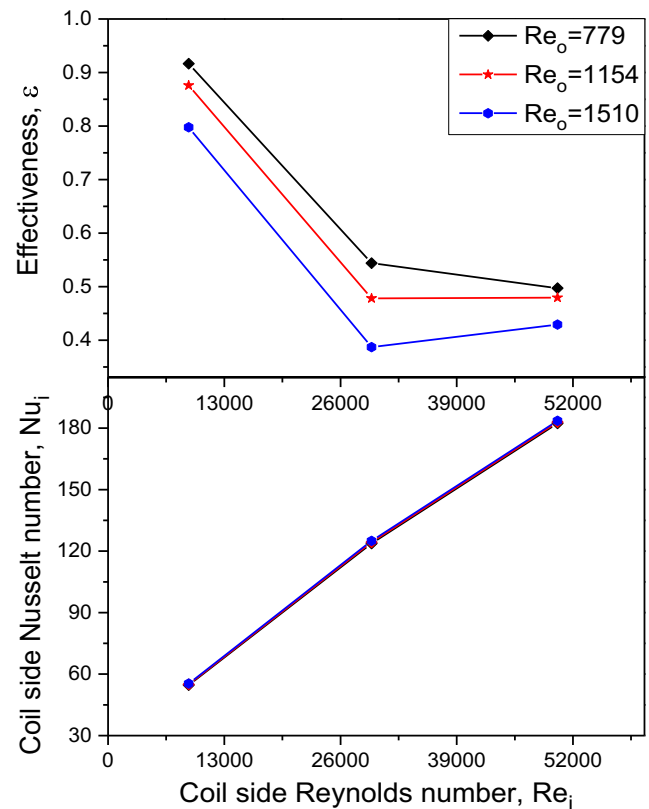


Fig. 12 Effect of coil side Reynolds number on thermal performance of the TFHE

coefficient with constant surface area compared to rise in  $C_{min}$  is less. As a result effectiveness of heat transfer from hot water to normal water decreases, which are in agreement with the result indicated in Fig. 12.

From Fig. 12, it is also observed that with increment in outer annulus side Reynolds number, effectiveness of heat transfer from coil side fluid to outer annulus side fluid decreases appreciably and coil side Nusselt number changes negligibly. Because, increased outer annulus side Reynolds number have little effect on mean temperature of heat rejection of hot water, coil side Reynolds number, prandtl number. As a result, coil side Nusselt number changes negligibly with little changes in coil side Reynolds number and Prandtl number for fixed curvature ratio. But at the same time, effectiveness decreases significantly with decrement in heat rejection rate from hot water to normal water.

### 5.3 Design parameters and pressure drop characteristics of the TFHE

Similar to heat transfer analysis, friction factor associated with different fluid flow is required to analyze for better prediction of pressure drop characteristics of the TFHE. For this purpose, coil side friction factor was analyzed against various design parameters. Hence three different non-dimensional design

parameters i.e. coil side Reynolds number, coil curvature ratio and non dimensional coil pitch were selected for this study and their effect on non-dimensional pressure drop characteristics of the TFHE i.e. coil side friction factor was assessed and presented as follows.

### 5.3.1 The effect of coil curvature ratio on pressure drop characteristics of the TFHE

The effect of coil side curvature ratio on pressure drop characteristics of the TFHE i.e. coil side friction factor,  $f_i$  were tested in the validated analytical model for three different coil side curvature ratio i.e. 0.091, 0.152 and 0.216 respectively and the results are represented graphically in Fig. 13 for counter flow configuration with respect to different coil side Reynolds number.

In this study, non-dimensional coil pitch and outer annulus side volumetric flow rate are taken as constant with respect to variation or increase in coil curvature ratio. It is observed from Fig. 13 that coil side friction factor increases with increment in coil curvature ratio. Because by increasing the coil curvature ratio with respect to a specific Reynolds number, coil side fluid velocity, equivalent diameter of helical coil, and mean temperature of heat rejection decreases, where as residence time of hot water increases. As coil side friction factor,  $f_i$  is dependent on numbers of parameters i.e. equivalent diameter,  $D_e$ , density of the fluid,  $\rho$ , fluid velocity,  $V$ , length of the coil,  $L_c$ , with small variation in these parameters coil side friction factor,  $f_i$  will change, which is also observed in Fig. 14 that coil side friction factor increases with increase in coil curvature ratio because of the collective effect of decreased fluid velocity, fluid density and equivalent diameter.

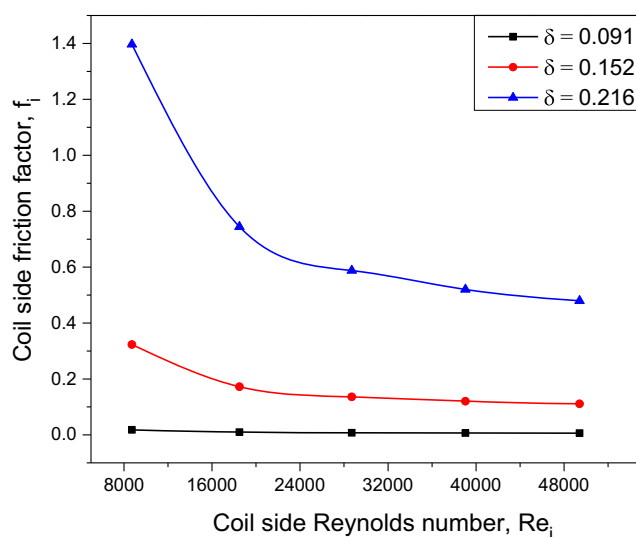


**Fig. 13** Effect of coil side Reynolds number and coil curvature ratio on coil side friction factor

### 5.3.2 The effect of non-dimensional coil pitch on pressure drop characteristics of the TFHE

The effect of non-dimensional coil pitch on pressure drop characteristics of the TFHE i.e. coil side friction factor,  $f_i$  were tested in the validated analytical model for three different non-dimensional coil pitches i.e. 0.083, 0.115 and 0.148 and the results are represented graphically with respect to coil side Reynolds number are shown in Fig. 14 for counter flow configuration.

In this study, coil curvature ratio and outer annulus side volumetric flow rate are taken as constant during the analysis with respect to variation or increase in non-dimensional coil pitch. It is observed from Fig. 14 that coil side friction factor increases with increment in non-dimensional coil pitch. Because with increment in non-dimensional coil pitch, helical coil length, heat transfer surface area, rate of heat rejection from hot water and residence time decreases, whereas mean temperature of heat rejection within the helical coil increases. As a result, coil side friction factor,  $f_i$  increases with increase in non-dimensional coil pitch due to the collective effect of decreased coil length, fixed tube size and fluid velocity corresponds to a specified coil side Reynolds number.

### 5.3.3 The effect of coil side Reynolds number on pressure drop characteristics of the TFHE

The effect of coil side Reynolds number on pressure drop characteristics of the TFHE i.e. coil side friction factor,  $f_i$  were tested in the validated analytical model for five different coil side Reynolds number i.e. 8723, 18,492, 28,704, 39,034 and 49,411 as well as the results are represented graphically in Figs. 13 and 14 for counter flow configuration. By increasing

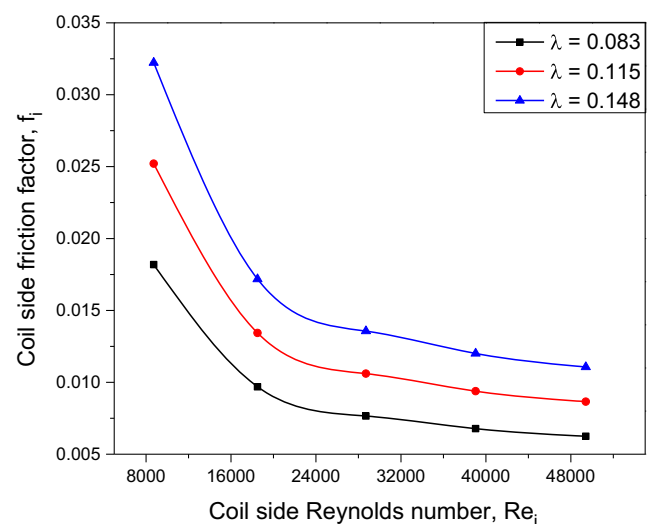


**Fig. 14** Effect of coil side Reynolds number and non-dimensional coil pitch on coil side friction factor

the coil side Reynolds number of hot water, coil side fluid velocity increases, whereas residence time of hot water inside the helical coil decreases. So the mean temperature of heat rejection and several thermo physical properties increases. It is observed from Figs. 13 and 14 that coil side friction factor,  $f_i$  decreases with increase in coil side Reynolds number due to the collective effect of increased fluid velocity and fluid density for fixed coil length and equivalent diameter.

#### 5.4 Optimum heat transfer enhancement condition

The calculated SNR or S/N ratios for 36 numbers of experiments are shown in Table 3. The contribution of each factor on thermal performance and pressure drop characteristics of the TFHE are presented in Table 5, where R is the difference between the maximum and minimum S/N ratio for each factor, Contribution ratio is the ratio of R value of any factor to the total R values of all factors and Rank represents the orderly assignment of factor with respect to maximum heat transfer and minimum pressure drop. Thermal performance parameters and pressure drop characteristics of the TFHE are dependent on numbers of factors i.e. mass flow rate of hot water, normal water and air, inlet temperature of hot water, geometric parameters of the helical coil, innermost copper tube and outermost mild steel tube etc. For this study, tube size, coil pitch, coil diameter and volumetric flow rate of hot water are considered as the key design parameters and Taguchi technique is used to determine the effect of these design parameters on thermal performance and pressure drop characteristics of the TFHE. The optimum condition is calculated for a combination of levels of control factors having largest S/N ratio.

The effect of each design parameters on Nusselt number,  $Nu_i$  is shown in Fig. 15. The optimum values of these design parameters for maximum heat transfer i.e. Nusselt number,  $Nu_i$  is obtained for  $d_{c,i} = 0.0045$  m,  $p = 0.018$  m,  $D_c = 0.04253$  m and  $\dot{V}_h = 5$  LPM according to “larger is the better” quality characteristics. Using optimum values of these parameters in analytical model, Nusselt number and friction

factor are calculated about 185.033 and 0.00865 respectively, which are shown in Table 6. The contribution ratio of each parameter on Nusselt number is shown in Fig. 17 and Table 5. It is clear from figure that the volumetric flow rate of hot water,  $\dot{V}_h$  is the most effective parameter on Nusselt number with a contribution ratio of 66.82% followed by tube size,  $d_{c,i}$ , coil diameter,  $D_c$  and coil pitch,  $p$  with the contribution ratio of 27.61, 4.27 and 1.29% respectively. It is observed from the results that coil diameter and coil pitches have least effect on coil side Nusselt number.

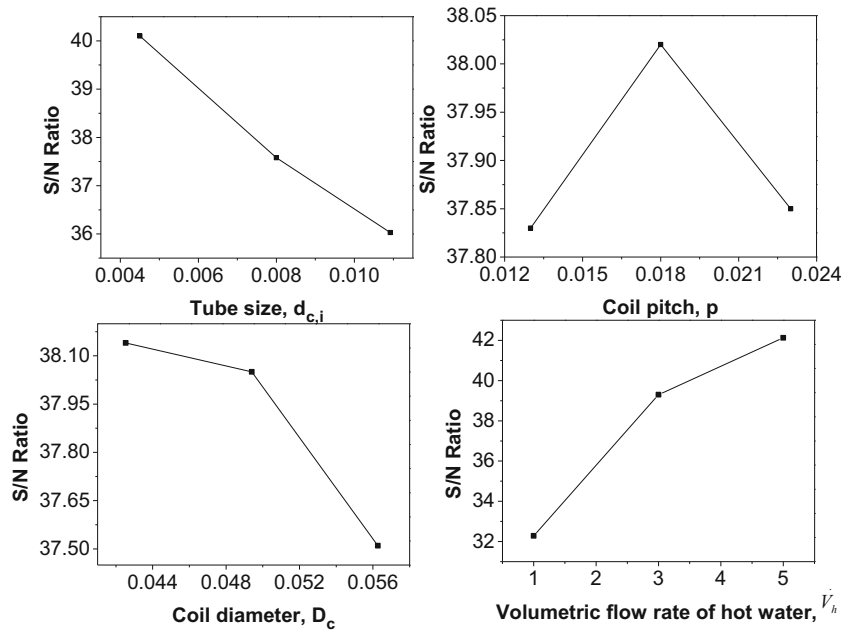
Similarly the effect of each design parameters on friction factor,  $f_i$  is shown in Fig. 16. The optimum values of these design parameters for minimum pressure drop i.e. friction factor,  $f_i$  is obtained for  $d_{c,i} = 0.0045$  m,  $p = 0.013$  m,  $D_c = 0.056266$  m and  $\dot{V}_h = 5$  LPM according to “smaller is the better” quality characteristics. Using optimum values of these parameters in analytical model, Nusselt number and friction factor are calculated about 175.729 and 0.00624 respectively, which are shown in Table 6. The contribution ratio of each parameter on friction factor is shown in Fig. 18 and Table 5. It is clear from figure that the parameter tube size,  $d_{c,i}$  is the most effective parameter on friction factor with a contribution ratio of 71.07% followed by volumetric flow rate of hot water,  $\dot{V}_h$ , coil pitch,  $p$  and coil diameter,  $D_c$  with the contribution ratio of 18.2, 9.19 and 1.52% respectively. It is observed from the results that coil pitch and coil diameters have least effect on friction factor.

Afterwards overall optimization process for the TFHE is carried out as per the statistical technique approached by Gunes et al. [16]. For overall optimization process it is required to combine the separate effects of each goal with respect to levels of importance of each parameter. Optimum conditions of each design parameters for coil side Nusselt number and coil side friction factor are determined  $[(d_{c,i})_1]^b [(p)_2]^d [(D_c)_1]^c [(\dot{V}_h)_3]^a$  and  $[(d_{c,i})_1]^a [(p)_1]^c [(D_c)_3]^d [(\dot{V}_h)_3]^b$  respectively. Here, 1, 2 and 3 represents the level of respective design parameters with respect to maximum S/N

**Table 5** Contribution of design parameters towards output responses

Contribution of design parameters of the TFHE on Nusselt number, $Nu_i$						Contribution of design parameters of the TFHE on friction factor, $f_i$					
	Level	$d_{c,i}$	$p$	$D_c$	$\dot{V}_h$		Level	$d_{c,i}$	$p$	$D_c$	$\dot{V}_h$
S/N Ratio	1	40.1	37.83	38.14	32.28	S/N Ratio	1	37.639	19.1984	16.2191	10.6236
	2	37.58	38.02	38.05	39.3		2	12.8304	16.6799	16.9144	19.1999
	3	36.03	37.85	37.51	42.13		3	-0.3039	14.2874	17.0322	20.3422
R		4.07	0.19	0.63	9.85	R		37.9431	4.911	0.8131	9.7186
Rank		2	4	3	1	Rank		1	3	4	2
Contribution Ratio %		27.61	1.29	4.27	66.82	Contribution Ratio %		71.07	9.19	1.52	18.2

**Fig. 15** Effects of each design parameter on coil side Nusselt number,  $Nu_i$



ratio and a, b, c and d represents the ranking order of the design parameters with respect to their contribution ratio as mentioned in Table 5. From Figs. 17 and 18 and Table 6, it is resulted that the first level of the tube size, coil pitch, coil diameter and the third level of the hot water flow rate is the general optimum condition of the design parameters  $(d_{c,i})_1(p)_1(D_c)_1(\dot{V}_h)_3$ . Because from  $[(d_{c,i})_1]^b$  and  $[(d_{c,i})_1]^a$ ,  $[(d_{c,i})_1]^a$ , from  $[(p)_2]^d$  and  $[(p)_1]^c$ ,  $[(p)_1]^c$ , from  $[(D_c)_1]^c$  and  $[(D_c)_3]^d$ ,  $[(D_c)_1]^c$  and from  $[(\dot{V}_h)_3]^a$  and  $[(\dot{V}_h)_3]^b$ ,  $[(\dot{V}_h)_3]^a$  are identified as the optimal design parameters with respect to ranking for this study.

### 6 Conclusions

In this study, an analytical investigation and performance optimization of the TFHE was performed. An analytical model

was prepared, validated against experimental result and researches mentioned in literature. Taguchi method was used for determination of optimum design parameters for maximum heat transfer and minimum pressure drop in TFHE. Out of several parameters, tube size,  $d_{c,i}$ , coil pitch,  $p$ , coil diameter,  $D_c$  and volumetric flow rate of hot water are considered as the key design parameters for the analysis along with effect of incoming air and normal water. The results of this work can be summarized as follows.

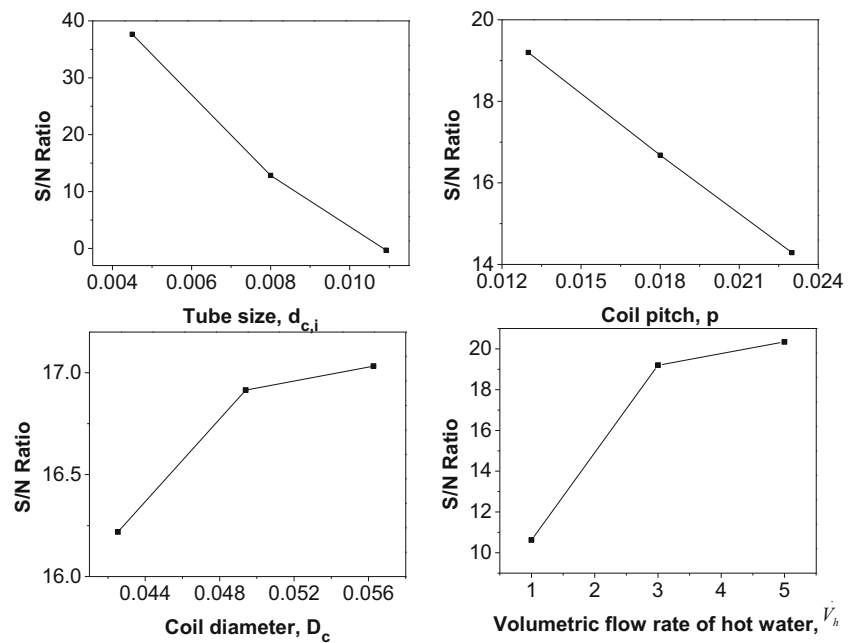
- i. For maximum heat transfer in TFHE, the optimum value of different design parameters were obtained as  $d_{c,i} = 0.0045$  m,  $p = 0.018$  m,  $D_c = 0.04253$  m and  $\dot{V}_h = 5$  LPM. For minimum pressure drop in TFHE, the optimum value of different design parameters were obtained as  $d_{c,i} = 0.0045$  m,  $p = 0.013$  m,  $D_c = 0.056266$  m and  $\dot{V}_h = 5$  LPM. Finally general optimization process for the TFHE was carried out by combining the effects of each design

**Table 6** Optimum conditions of design parameters and magnitude of performance parameters

		Parameters				Tested Nusselt number, $Nu_i$	Tested Friction factor, $f$
		$d_{c,i}$ , m	$p$ , m	$D_c$ , m	$\dot{V}_h$ , LPM		
Nusselt number	Optimum level	1 <sup>b</sup>	2 <sup>d</sup>	1 <sup>c</sup>	3 <sup>a</sup>	185.033	0.00865
	Optimum value	0.0045	0.018	0.04253	5		
Friction factor	Optimum level	1 <sup>a</sup>	1 <sup>c</sup>	3 <sup>d</sup>	3 <sup>b</sup>	175.729	0.00624
	Optimum value	0.0045	0.013	0.056266	5		
General	Optimum level	1	1	1	3	183.041	0.00816
	Optimum value	0.0045	0.013	0.04253	5		



**Fig. 16** Effects of each design parameter on coil side friction factor,  $f_i$



parameters and the optimum value of different design parameters were obtained as  $d_{c,i} = 0.0045$  m,  $p = 0.013$  m,  $D_c = 0.04253$  m and  $\dot{V}_h = 5$  LPM.

- ii. Contribution ratios of each design parameter on heat transfer and pressure drop were determined. Volumetric flow rate of hot water is found out the most effective parameter affecting heat transfer with a contribution ratio of 66.82% followed by tube size, coil diameter and pitch and tube size with 27.61, 4.27 and 1.29% contribution ratio respectively. Tube size is found out the most effective parameters affecting pressure drop with a contribution ratio of 71.07% followed by volumetric flow rate of hot water, coil pitch and coil diameter 18.2, 9.19 and 1.52% respectively.

- iii. The effect of three non dimensional design parameters i.e. coil curvature ratio, non-dimensional coil pitch and coil side Reynolds number on thermal performance i.e. coil side Nusselt number,  $Nu_i$  and effectiveness,  $\varepsilon$  and pressure drop characteristics i.e. coil side friction factor,  $f_i$  are tested in the validated analytical model of the TFHE. From result it is observed that with rise in curvature ratio and coil side Reynolds number, heat transfer effectiveness from helical coil increases, whereas coil side Nusselt number and friction factor decreases. Unlikely, with rise in non-dimensional coil pitch, heat transfer effectiveness from helical coil and coil side friction factor decreases, whereas coil side Nusselt number increases.

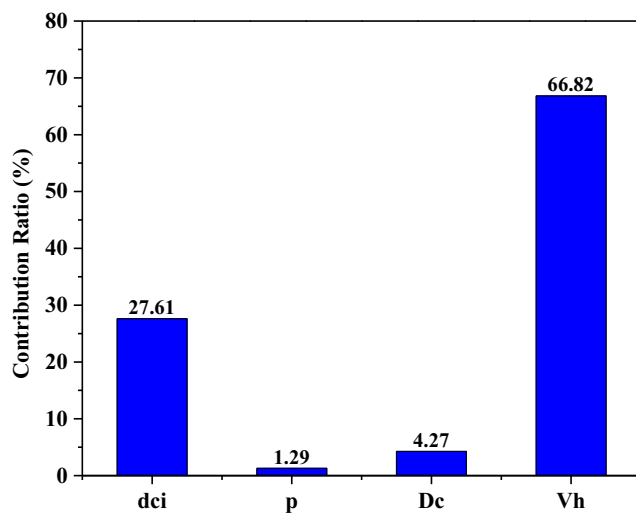


**Fig. 17** Contribution ratio of each design parameter to coil side Nusselt number,  $Nu_i$

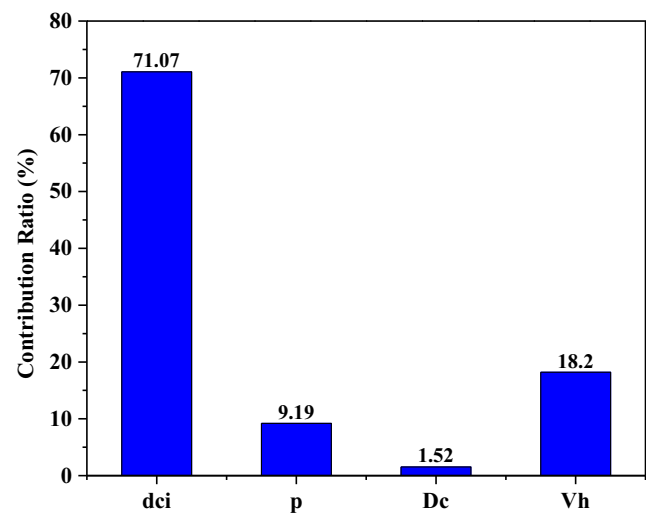


**Fig. 18** Contribution ratio of each design parameter to coil side friction factor,  $f_i$

- iv. Development of Nusselt number correlations having Dean number, Reynolds number, Prandtl number and curvature ratio for helical coil side and outer annulus side fluid may be carried out in future for generic use. Nusselt number correlations having Dean Number without Wilson plot method may be used for performance analysis of TFHE in future.

### Compliance with ethical standards

**Conflict of interest** On behalf of all authors, the corresponding author states that there is no conflict of interest.

### Appendix

Thermo physical properties of various fluid used.

For water: [28]

$$\begin{aligned}\rho(T) &= 0.257 + 16.864T - 0.105T^2 + 3.229 \times 10^{-4}T^3 \\ k(T) &= 0.284 + 0.001T + 1.673 \times 10^{-14}T^2 \\ c_p(T) &= 4.109 + 2.197 \times 10^{-4}T - 8.563 \times 10^{-14}T^2 \\ \mu(T) &= 0.0035 - 9.156 \times 10^{-6}T - 1.175 \times 10^{-16}T^2 \\ Pr(T) &= 24.883 - 0.065T - 6.515 \times 10^{-13}T^2\end{aligned}$$

For air: [29]

$$\begin{aligned}\rho(T) &= 36.238 - 0.214T - 9.158 \times 10^{-5}T^2 + 2.599 \times 10^{-6}T^3 \\ k(T) &= -0.148 + 0.001T + 4.106 \times 10^{-7}T^2 \\ c_p(T) &= 1.504 - 0.003 \times 10^{-4}T - 1.368 \times 10^{-6}T^2 \\ \mu(T) &= -6.701 \times 10^{-5} + 4.886 \times 10^{-7}T + 1.916 \times 10^{-10}T^2 \\ Pr(T) &= 3.805 - 0.019T - 8.213 \times 10^{-6}T^2\end{aligned}$$

**Publisher's Note** Springer Nature remains neutral with regard to jurisdictional claims in published maps and institutional affiliations.

### References

- Shokouhmand H, Salimpour MR, Akhavan-Behabadi MA (2008) Experimental investigation of shell and coiled tube heat exchangers using Wilson plots. *Int Commun Heat Mass Transf* 35:84–92
- Batmaz E, Sandeep KP (2005) Calculation of overall heat transfer coefficients in a triple tube heat exchangers. *Heat Mass Transf* 41: 271–279
- Rennie TJ, Raghavan VGS (2005) Experimental studies of a double-pipe helical heat exchanger. *Exp Thermal Fluid Sci* 29: 919–924
- Pawar SS, Sunnapwar VK (2013) Experimental studies on heat transfer to Newtonian and non-Newtonian fluids in helical coils with laminar and turbulent flow. *Exp Thermal Fluid Sci* 44:792–804
- Zhang H, Shao S, Xu H, Zou H, Tang M, Tian C (2016) Numerical investigation on fin-tube three-fluid heat exchanger for hybrid source HVAC & R systems. *Appl Therm Eng* 95:157–164
- Pătrășcioiu C, Rădulescu S (2015) Prediction of outlet temperatures in triple concentric-tube heat exchangers in laminar flow regime: case study. *Heat Mass Transf* 51:59–66
- Boultif N, Vougriou C (2017) Steady and unsteady state thermal behavior of triple concentric-tube heat exchanger. *Heat Mass Transf* 53:849–863
- Alimoradi A, Veysi F (2017) Optimal and critical values of geometrical parameters of shell and helically coiled tube heat exchangers. *Case Stud Therm Eng* 10:73–78
- Omid M, Farhadi M, Jafari M (2017) A comprehensive review on double pipe heat exchangers. *Appl Therm Eng* 110:1075–1090
- Dizaji HS, Khalilarya S, Jafarmadar S, Hashemian M, Khezri M (2017) A comprehensive second law analysis for tube-in-tube helically coiled heat exchangers. *Exp Thermal Fluid Sci* 76:118–125
- Gomaa A, Halim MA, Elsaid AM (2017) Enhancement of cooling characteristics and optimization of a triple concentric-tube heat exchanger with inserted ribs. *Int J Heat Therm Sci* 120:106–120
- Unal A (1998) Theoretical analysis of triple concentric-tube heat exchangers, part-1: mathematical modelling. *Int Commun Heat Mass Transf* 25:949–958
- Unal A (2001) Theoretical analysis of triple concentric-tube heat exchangers, part-2: case studies. *Int Commun Heat Mass Transf* 28: 243–256
- Mohapatra T, Padhi BN, Sahoo SS (2017) Experimental investigation of convective heat transfer in an inserted coiled tube type three fluid heat exchanger. *Appl Therm Eng* 117:297–307
- Sekulic DP, Shah RK (1995) Thermal design theory of three fluid heat exchangers. *Adv Heat Tran* 26:219–329
- Jamshidi N, Farhadi M, Ganji DD, Sedighi K (2013) Experimental analysis of heat transfer enhancement in shell and helical tube heat exchangers. *Appl Therm Eng* 51:644–652
- Rose JW (2004) Heat-transfer coefficients, Wilson plots and accuracy of thermal measurements. *Exp Thermal Fluid Sci* 28:77–86
- Gnielinski V (1976) New equation for heat and mass transfer in turbulent pipe and channel flow. *Int Chem Eng* 16:359–368
- Seban RA, McLaughlin EF (1963) Heat transfer in tube coils with laminar and turbulent flow. *Int J Heat Mass Transf* 6:387–395
- Rogers GFC, Mayhew YR (1964) Heat transfer and pressure loss in helically coiled tube with turbulent flow. *Int J Heat Mass Transf* 7: 1207–1216
- Kalb CE, Seader JD (1972) Heat and mass transfer phenomena for viscous flow in curved circular pipe. *Int J Heat Mass Transf* 15: 801–817
- Mishra P, Gupta SN (1979) Momentum transfer in curved pipes: Newtonian fluids. *Ind Eng Chem Des Dev* 18:130–137
- Coates J, Pressburg BS (1959) Heat transfer to moving fluids. *Chem Eng* 28:67–72
- Blasius H (1908) Grenzschichten in Flüssigkeiten mit kleiner Reibung (German). *Z Math Phys* 56:1–37
- Etghani MM, Baboli SAH (2017) Numerical investigation and optimization of heat transfer and exergy loss in shell and helical tube heat exchanger. *Appl Therm Eng* 121:294–301
- Gunes S, Manay E, Senyigit E, Ozceyhan V (2011) A Taguchi approach for optimization of design parameters in a tube with coiled wire inserts. *Appl Therm Eng* 31:2568–2577
- Jamshidi N, Farhadi M, Sedighi K, Ganji DD (2012) Optimization of design parameters for nanofluids flowing inside helical coils. *Int Commun Heat Mass Transf* 35:84–92
- [www.me.ua.edu/me215/f07.woodbury/ExcelStuff/XSteam-v2a.xlsm](http://www.me.ua.edu/me215/f07.woodbury/ExcelStuff/XSteam-v2a.xlsm). Accessed 3 Nov 2017
- [https://www.mne.psu.edu/cimbala/me433/Links/Table\\_A\\_9\\_CC\\_Properties\\_of\\_Air.pdf](https://www.mne.psu.edu/cimbala/me433/Links/Table_A_9_CC_Properties_of_Air.pdf). Accessed 3 Nov 2017